Journal of Engineering Science and Technology
4th EURECA 2015 Special Issue February (2016) 113 - 128

INVESTIGATION OF THE COFFEE WASTE-DERIVED ADSORBENT

Y. N. CHAIW, K. K. ANG, T. LEE, XIAO Y. LIM*

Energy Research Group, School of Engineering, Taylor's University, Taylor's Lakeside Campus, No. 1 Jalan Taylor's, 47500, Subang Jaya, Selangor DE, Malaysia
*Corresponding Author: xiaoyien.lim@taylors.edu.my

Abstract

Due to the rapid development in the industrial sector, the concentration of carbon dioxide (CO_2) in the atmosphere has increased by 30% over the years. Hence, low-cost activated carbon derived from coffee waste for the application of carbon capture and sequestration technology has been proposed in curbing the devastating effect cause by CO_2 emission. The activated carbon was treated with different chemical activating agent such as potassium hydroxide and potassium carbonate at two different chemical concentration which were 20 and 50 wt. %, in order to study the effect of the different chemical agent and concentration towards the evolution of microporosity structure and surface chemistry that is desired to be used in CO_2 adsorption application. A series of characterization were performed on the activated carbon by using Brunauer-Emmett-Teller (BET), Fourier Transform Infrared Spectroscopy (FTIR) and Thermogravimetric analysis (TGA). The result shows that 50 wt. % of potassium carbonate activation appears to be the best combination for the structural development and higher CO_2 adsorption performance.

Keywords: Adsorption, Activated carbon, Carbon dioxide, Carbonization.

1. Introduction

Over the years, the intense development of modern civilization has led to the rapid depletion of fossils fuels energy resources such as coal. Extensive utilization of fossil fuels has resulted in the secretion of huge amount of carbon dioxide (CO_2) gases into the atmosphere which lead to the phenomenon of global climate change [1]. In fact, over 30 billion tons of CO_2 is emitted into the atmosphere in an annual basis [2]. From a research study by the International Panel on Climate Change (IPCC), it is anticipated that the average CO_2 concentration in the atmo-

Nomenclatures

CO_2	Carbon Dioxide
K_2CO_3	Potassium Carbonate
KOH	Potassium Hydroxide
N_2	Nitrogen
wt. %	Weight Percent

Abbreviations

AC	Activated Carbon
BET	Brunauer-Emmett-Teller
CCS	Carbon Capture and Sequestration
FTIR	Fourier Transform Infrared Spectroscopy
IPCC	International Panel on Climate Change
PSD	Pore Size Distribution
TGA	Thermogravimetric Analyser

sphere may upsurge to 570 ppm by the year of 2100 which will cause an increase in global average temperature and mean sea level by 1.9°C and 3.8 m respectively [3]. Thus, great deal of efforts has to be devoted in order to limit the emissions of CO_2 into the atmosphere within an adequate level. Carbon capture and sequestration (CCS) technology from point source emissions has emerged as one of the potential solution in stabilizing the concentration of CO_2 in the atmosphere by 85% or more [4]. The captured CO_2 gas not only able to reduce the effect of global warming but it also can be utilized in oil recovery where CO_2 gas is injected into the declining oil field in order to increase the amount of crude oil that can be extracted out from oil fields [5].

In general, CCS has three main approaches which are pre-combustion, post-combustion and oxy-fuel combustion [4]. Although CCS technology is an effective technique in curbing the effect of global warming, unfortunately, the cost in CO_2 capture phase are relatively high, which makes up 50-80% of the overall cost of CCS technology [6]. Thus, it is vital to reduce the overall cost of CCS technology in order to create a more economical viable technology. From previous research studies, post combustion capture of CO_2 possess great potential in reducing the overall cost of CCS technology [4]. Till date, most of the industrial sector utilizes amine-based processes in capturing the CO_2 gases emitted due to higher selectivity as well as CO_2 capturing efficiency. However, this technique is costly, energy intensive as well as large amount of water supply was needed during the process and it causes corrosion to equipment due to amine degradation [7]. Hence, the major challenge in current research is to develop a cost-effective as well as environmentally friendly technology for CO_2 capture.

As an alternative, gas-solid adsorption has been taken into consideration as it exhibits numerous advantages such as reduction in cost, increased the carrying capacity of CO_2, low energy regeneration, minimal pressure drop compared to other technologies, rapid reaction rates and the ease of applicability over a wide range of temperatures and pressures [7, 8]. However, the success of this approach is highly dependent on the capability in developing an adsorbent that can be easily regenerated and durable with high CO_2 selectivity as well as adsorption capacity. Among the various type of adsorbents available in the market, activated carbon (AC) has been chosen as a promising and cost-effective adsorbent due to its

natural characteristics such as large pore volume, high surface area and reactivity, hydrophobicity in nature, high adsorption capacity, wide availability and minimal initial cost [7, 9]. Unfortunately, the commercial AC is generally derived from fossil fuels, which thought to be less environmental friendly. Thus, this has initiated the need in searching for sustainable carbonaceous resources in producing AC such as lignocellulosic biomass.

Over the years, much attempts have been made in developing AC from numerous range of biomass such as rice husk, rubber-wood sawdust, oil palm shell and tea waste [10, 11]. However, the use of coffee waste as a biomass precursor in producing AC for CO_2 adsorption has yet to gain the attention of the society. Hence, in this research study, coffee waste has been selected as the precursor in the production of AC. The selection of coffee waste as a precursor in the production of AC is mainly due to its abundance in supply as well as rich in crude fibre content (lignin, cellulose and hemicellulose) as studies have shown that approximately 50% of the coffee waste composition comprises of carbon [12]. The rich carbon content in coffee waste makes it a suitable precursor in producing AC with desirable properties that can be used in CCS technology.

Past research shown that the formation of micropores structure and high surface area were the main key element in maximizing the CO_2 adsorption efficiency which was influenced by the type of chemical activating agent as well as chemical concentration used during the activation process [13]. In this research study, the objective is to study the effect of potassium hydroxide (KOH) and potassium carbonate (K_2CO_3) concentrations (50 wt. % and 20 wt. %) on the surface chemistry, textural properties as well as CO_2 adsorption performance of the coffee waste derived AC. The adsorption performance of the AC produced was analyzed by using the Thermogravimetric Analyser (TGA); Fourier Transform Infrared Spectroscopy (FTIR) to analyse the surface chemistry and Brunauer, Emmett and Teller (BET) to analyse the microporosity structure of the AC.

2. Materials and Methods

2.1. Materials

Raw coffee waste was sponsored by Starbucks in Taylor's University Lakeside Campus, Subang Jaya, Malaysia. In the preparation of AC from coffee waste, KOH and K_2CO_3 of analytical grade purchased from Malaysia R&M Chemicals Ltd. were used as chemical activating agent during the activation process. The final end product obtained was stored inside a desiccator containing silica gel in order to prevent the formation of water vapor in the sample.

2.2. Pre-treatment of coffee waste

The coffee waste was first washed with distilled water in order to remove the impurities present on the surface before undergoes further treatment. The coffee waste were then dried inside the oven for 24 hours at 110^{o}C [14, 15] to remove the moisture content so that the growth of fungal which will eventually affect the efficiency of the AC produced can be avoided. After drying, the dried coffee waste was stored in a cool, dry place.

2.3. Carbonization process

Carbolite furnace (Model: HST 12/400) was used to perform the carbonization and activation process for the production of AC from coffee waste. Approximately 30 gram of dried coffee waste was placed in a ceramic boat and was positioned in the centre of the constant temperature zone of the ceramic tubing in the horizontal tube furnace. The ceramic tubing containing the samples in the ceramic boat was flowed with continuous N_2 gas with a constant flow rate of 1 L/min for 1 hour in order to eliminate the oxygen content inside the tubing. After 1 hour, the sample was heated to 800°C with heating rate of 20°C/min under a constant flow of N_2 gas for 1 hour upon reaching the desired temperature. The sample was allowed to cool to 100°C after the completion of heating process before it was removed from the furnace.

2.4. Physiochemical activation process

The carbonized char produced via carbonization was impregnated with 50 wt. % of KOH with an impregnation ratio of 1:1, where 100 gram of KOH was diluted with 100 ml of distilled water. 30 ml of KOH solution was later extracted from the mixture and was then impregnated with the carbonized char in order to obtain an impregnation ratio of 1:1. The impregnated sample was stirred at 300 rpm with a magnetic stirrer for 1 hour for complete impregnation. Once the chemical activation has completed, the sample was filtered with filter paper and washed repeatedly with distilled water until a constant pH of 7 was obtained. Similar procedure was repeated for a chemical concentration of 20 wt. % where 25 gram of KOH was diluted with 100 ml of distilled water.

The sample prepared via chemical activation was placed back into the horizontal tubular furnace to be heated up to a desired temperature of 700°C under a constant flow of CO_2 gas with similar flow rate and heating rate for 1 hour. The sample was cool to 100°C before it was being discarded from the furnace. After removing the sample from the furnace, the AC sample was stored in a sealed sample flask in a cool, dry environment and was assigned with sample codes as shown in Table 1. Similar procedure was repeated for chemical concentration of 50 wt. % and 20 wt. % for K_2CO_3 as the chemical activating agent instead on KOH.

Table 1. Samples code for raw and activated carbon.

Sample	Sample ID
Raw coffee waste	RCW
Carbonized char (without chemical treatment)	CCW
Chemical Activation with 20 wt. % KOH solution	KH2
Chemical Activation with 20 wt. % K_2CO_3 solution	KC2
Chemical Activation with 50 wt. % KOH solution	KH5
Chemical Activation with 50 wt. % K_2CO_3 solution	KC5

2.5. Characterization and analysis of AC

2.5.1. Proximate analysis

Proximate analysis was performed using TGA Analyser (Model: Settaram TGA92) which is located in Nottingham University, Malaysia. The moisture level, ash content, fixed carbon and volatile matter content in the raw coffee waste sample was determined. In an inert condition, approximately 15 mg of raw coffee waste sample was heated to 110°C with a heating rate and flow rate of 10°C/min and 50 ml/min respectively. The sample was heated isothermally for 20 minutes for complete dehydration. Later, the temperature was ramped up to 950°C and was held isothermally for 30 minutes to eliminate the volatile matters from the sample. N_2 gas was then replaced with air and was held constant at 950°C for another 20 minutes to promote combustion process, leaving only the ash. The sample was cool to a temperature of 100°C before it was being removed.

2.5.2. Thermogravimetric analysis for CO_2 adsorption

CO_2 adsorption of coffee waste derived AC was analyzed by using Thermogravimetric (TGA) Analyser (Model: Settaram TGA92) which is located in Nottingham University, Malaysia. Under a constant flow of N_2 gas, approximately 15 mg of sample was placed in a crucible and was heated up to a desired temperature of 60°C with a flow rate and heating rate of 50 ml/min and 10°C/min respectively. The sample was heated isothermally at 60°C for 30 minutes. After 30 minutes, the N_2 gas was replaced with a continuous flow of CO_2 gas under the same temperature and flow rate for another 90 minutes. After completion of the adsorption phase, desorption phase was carried out where CO_2 gas was replaced back with N_2 and was allowed to flow for another 30 minutes under the same operating conditions [16].

2.5.3. Fourier transform infrared spectroscopy (FTIR) analysis

FTIR analysis was performed in order to study the active carbon surface functional groups of the prepared samples. The equipment used for the FTIR analysis was Perkin Elmer Spectrum 100 FTIR Spectrometer equipped with a software named, Spectrum. The discs were prepared by first mixing a small amount of sample at a ratio of 1:99 with KBr powder in an agate mortar. The resulting mixture was placed into a hydraulic press for pelletizing with a force of 10 tons at vacuumed pressure for approximately 30 seconds. The sample was then placed onto a disc holder and it was measured using the FTIR Spectrophotometer. The FTIR spectra were recorded between a wavelengths of 4000 to 650 cm^{-1} [17].

2.5.4. Brunauer-Emmett-Teller (BET) analysis

The total surface area of the AC produced was determined by N_2 adsorption isotherm at 77 K by using Micromeritics ASAP 2020 Analyzer. The samples were degassed for 6 hours under vacuum condition at 130°C prior analyzing process. A relative pressure (P/P_o) range of 0-1.0 for the adsorption data was used in determining the total surface area by utilizing the standard BET method [18].

The textural properties such as specific surface area, micropore volume and pore size distribution were calculated from the N_2 adsorption isotherms by using Brunauer-Emmett-Teller (BET), Dubinin-Radushkevich (DR) and Density Functional Theory (DFT) models, respectively [19].

3. Results and Discussion

3.1. Proximate analysis for raw coffee waste sample

Figure 1 illustrates the thermal degradation behaviour of the RCW sample where it can be generally categorized into three main regions which are, (i) the dehydration of water vapour, (ii) decomposition of hemicellulose and cellulose and (iii) decomposition of lignin and char [20]. From Fig. 1, a minor weight loss of 3.6% can be observed at the temperature of around 150°C which is attributed to the removal of water vapour physisorbed within the micropores structures [19]. The low evaporation of water vapour is mainly due to the adsorption of low water content from the surrounding environment by the hydrophobic surface of RCW. Even after the initial drying process at 110°C for 24 hours, a small amount of water molecules are still present on the surface of the biomass. However, only 3.6% of moisture content was observed from the TGA profile.

The subsequent degradation event happened at a temperature of approximately 200-560°C where thermal depolymerisation of hemicellulose and cellulose and partial lignin decomposition occurred. The decomposition of the lignin structure continued to have a gradual weight loss at the temperature beyond 560°C. In the temperature range of 280-480°C, hemicellulose and cellulose experienced a rapid decomposition which causes the drastic decrease in the TGA profile. This was due to the decomposition of aromatic compounds in the lignin structure as well as the regular decomposition of secondary organic residues [19]. While the wide range of lignin degradation which occurred at a temperature of 560-960°C is resulted from the decomposition of benzene ring. Benzene ring has a chemical structure that is harder to decompose, hence, it exhibit a slower decomposition rate as compared to hemicellulose and cellulose [19, 21]. This trend was verified in the past studies conducted by other researches as well [22-25]. Adding to that, the decomposition of hemicellulose and cellulose as well as partial lignin decomposition represents the amount of volatile matter containing in the RCW sample. From the TGA profile, a volatile content of 83.59% was obtained.

From Fig. 1, a fixed carbon content of 7% was obtained at 950°C. Temperature beyond 950°C initiates the total decomposition of lignin structure which results in ash formation. Thus, in this research work, the carbonization process was carried out at 800°C as literature studies conducted indicates that the optimum carbonization temperatures happened at the temperature range of 500-900°C [26]. Temperature beyond 900°C will results in the hardening of carbon structure which is due to the partial alignment of graphitic planes and eventually result in a decrease in porosity of the AC produced [27].

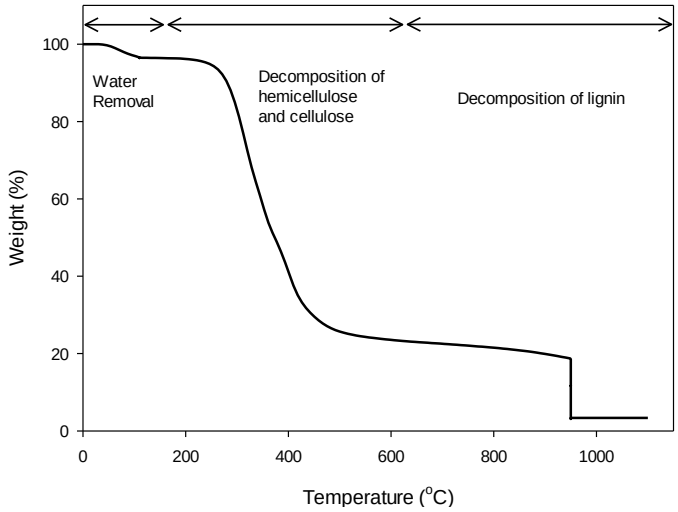

Fig. 1. Thermal decomposition of RCW sample.

3.2. CO_2 adsorption performance for activated carbon

The CO_2 adsorption profile for two different activating agent as well as chemical concentration (KH2, KH5, KC2 and KC5) was illustrated as shown in Fig. 2. Based on Fig. 2, all four samples exhibit a similar trend whereby a rapid increase in CO_2 adsorption capacity can be observed during the initial 60 minutes, and subsequently remains constant until the saturation point is achieved. The drastic increase in adsorption rate was initiated by the interaction between the adsorbent surface areas with the CO_2 molecules. Beyond 60 minutes, a reduction in active sites occurred and hence slower adsorption rate was observed. Rashidi et al. [28] and Li et al. [29] reported that the rapid adsorption during the initial stage was most likely due to the external surface of the adsorbent and subsequently followed by the slower diffusion process that happens internally. The flue gas temperature in post-combustion process is ranging at a temperature of 40-60°C [28, 30]. Hence, the CO_2 adsorption analysis performed in this study was conducted at a temperature of 60°C.

From Fig. 2, KC5 obviously demonstrated a higher CO_2 uptake which was of 2.6 wt. % as compared to the other three samples, KH2, KH5 and KC2 which only have a CO_2 uptake of 2.4, 2.3 and 2.3 wt. % respectively. The results indicate that chemical impregnation with K_2CO_3 at higher chemical concentration yield AC with better CO_2 adsorption performance as compare to KOH. Researcher concluded that the variation in CO_2 adsorption performance might be due to the amount of micropores structures formed within the AC which resulted from the chemical effects happening inside the pores [19, 31, 32]. It was reported that AC with high micropores structure will promote better adsorption capacity [19] which conforms to one of the research study done by Ludwinowicz and Jaroniec [33].

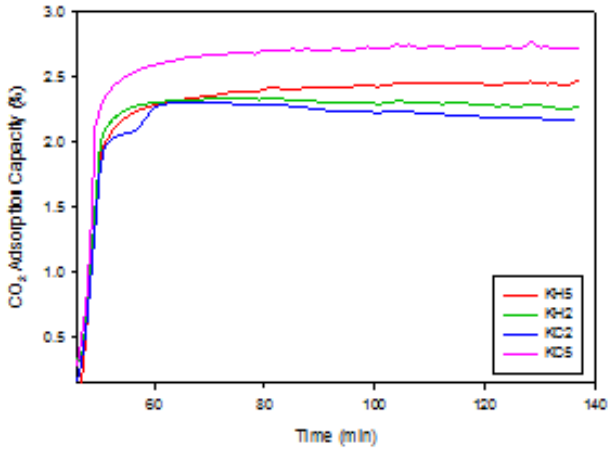

Fig. 2. CO_2 adsorption capacity curve for all AC.

3.3. FTIR analysis

Adsorption capacity in AC is highly dependent upon its porosity as well as chemical reactivity of functional groups at the surface. This reactivity initiates a discrepancy between forces at the surface, and thus leading to molecular adsorption by the Van der Waals forces. Knowledge on surface functional group would benefit in determining the adsorption capability of the AC produced. Past research studies conducted indicates that the presence of oxygen containing functional group such as carboxylic, lactone, phenol, carbonyl and ether plays important role in influencing the surface properties and adsorption behavior of the AC produced [7, 34, 35]. The presence of the oxygen functional group will initiate the bonding between the adsorbent and adsorbate [14]. Figure 3 illustrates the infrared spectra of six samples (RCW, CCW, KH2, KH5, KC2 and KC5). The more intense bands of the samples are as shown in Table 2. The FTIR spectra as illustrated in Fig. 3 clearly show the change in spectrum of the six samples. There were a few significant peaks that can be observed for RCW sample, mainly at 3400, 2925, 2854, 1745, 1649, 1390, 1378, 1163 and 1059 cm^{-1} which were assigned to O–H stretching vibration, C–H alkane group, C=O groups (usually presence in the carbonyl and lactones structures), N=O bending vibration and C–O stretching vibration of esters, respectively. The spectrum also revealed two other peaks at the adsorption band of 840 and 758 cm^{-1} which is directly attributed to the bending vibration of C–Cl alkyl halides groups (usually situated at the edge of the aromatic ring) [18].

The introduction of heat and different chemical activating agent as well as chemical concentration during the chemical treatment has resulted in the variation in spectrum to the raw biomass sample. A broad band of 3192 to 3236 cm^{-1} can be observed for CCW, KH2 and KC5 samples which can be characterized to the stretching vibration of hydroxyl groups. The presence of the hydroxyl stretching compound demonstrates that all the samples except for KC2 and KH5 samples shows strong hydrogen bond linkage. From Fig. 3, RCW, CCW, KH2 and KC5 spectra exhibit obvious peak frequency while KH5 and KC2 samples portrays a

smooth curve that no obvious peaks can be seen. This phenomenon was due to the elimination of oxygen functional groups or the damage done to the chemical structure of the sample due to either high chemical treatment or the type of chemical activating agent used. Past research studies conducted indicate that the change in surface chemistry, adsorption capacity and textural properties of the AC produced were influenced by the kind of chemical activating agent used as well as the concentration of the chemical agents [36, 37]. The presence of oxygen functional group is vital in contributing to the formation of high microporosity structure in AC. Oxygen containing functional group that is being removed will results in a change of linkage between aliphatic and aromatic bond. In other words, destruction in crosslink and the change in arrangement of the carbon layer will occur which will caused a collapse in the porosity structure within the AC [38, 39].

By comparing CCW with KH2 and KC5 samples, KH2 and KC5 samples which have undergo complete activation process show a slightly stronger hydrogen bond linkage. This indicates that the sample has undergoes a higher dehydration properties compares to CCW [40]. Although C-H stretching vibration in aromatics exists in all the samples, however, their transmittance intensities were rather weak with a broad wavelength. This is mainly due to the presence of water molecules in the samples [41, 42]. As AC has high absorption capabilities, the sample tends to absorb water vapour from the environment which leads to the high moisture level within the samples. KH2, KC5 and CCW samples demonstrate a spectrum that is almost similar. However, when comparing the spectrum for all six samples, most of the peaks have deviated from their initial frequency level or in some conditions, certain functional groups weakens and even disappear at certain concentration level of KOH and K_2CO_3 solution. For instance, the stretching vibration of esters group in RCW sample has weakens after undergo treatment process. On top of that, the alkyl hallides group which is initially absence in the raw biomass sample has formed at the adsorption band of 840 and 758 cm^{-1} after undergoing carbonization and activation process. A similar trend was observed in some of the previous research work done by other researches where some peaks were shifted or even disappeared when comparing with the spectrum of the raw biomass [14, 40]. It was concluded that this phenomena may be due to the destruction done to the lignin structure of some of the functional groups after it has undergo thermal and chemical treatment [14].

Table 2. Infrared bands for raw and activated carbons.

Wavelength (cm^{-1})	Type of Vibration	Functional Group Name
3400	ν (O – H)	Phenols & Alcohols
2925, 2854	ν (C – H)	Alkanes
1745, 1649	ν (C = O)	Carbonyl Compounds
1390, 1378	δ (N = O)	Nitro Group
1163, 1059	ν (C – O)	Esters
840, 758	γ (C – Cl)	Alkyl Hallides

[a] ν: stretching vibration
[b] δ: bending vibration (in-plane)
[c] γ: bending vibration (out-of-plane)

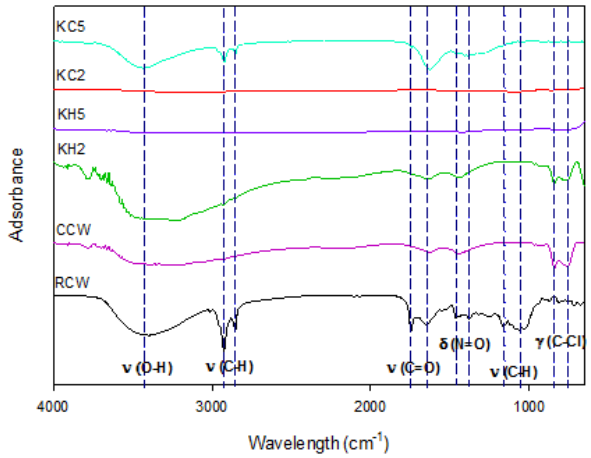

Fig. 3. FTIR spectra for raw and activated carbon.

3.4. Textural properties of AC

The adsorption performance of the AC are govern by several factors such as the active surface areas, pore sizes as well as the type of pores formed [19]. Particularly, the formation of micropores structure will able to yield AC with better CO_2 adsorption performance [18, 19]. Figure 4 shows the adsorption isotherm for KH2, KH5, KC2 and KC5 samples which were analyzed through physical adsorption of N_2 at 77 K. A sharp knee was observed at $P/P_o < 0.1$ for all four samples which indicates that the samples exhibited type 1 isotherm where the products were composed predominantly of well-developed micropores [18, 19]. From Fig. 4, KC5 shows the highest N_2 uptake as compared to the other three samples. This indicates that KC5 demonstrate a stronger interaction in the initial uptake for monolayer coverage, followed by micropores filling than the other three samples. From the N_2 adsorption curve, it was observed that a plateau was not achieved towards the tail of the curve for all four samples at $P/P_o > 0.6$. There was an increase in N_2 uptake at higher partial pressure region which shows an indication that there was a certain amount of mesopores structures presence the four samples [18, 43]. This results conforms to Table 3 where a mesopore volume of 0.0034, 0.003, 0.00034 and 0.023 cm^3/g were obtained for KH2, KH5, KC2 and KC5 samples respectively. Reffas et al. [44] and Sun et al. [43] have also reported similar trend in adsorption curve where at higher partial pressure region, there was an increase in N_2 uptake which shows the presence of mesopores structure.

Figures 5, 6 and 7 show the pore size distribution (PSD) for KH2, KH5 and KC5 samples respectively. While for KC2, the PSD profile could not be detected which most likely may be due to the limited amount of pores structure formed. The PSD profile for the three samples was computed by utilizing the density functional theory (DFT) model. For both KH2 and KH5 samples, a major peak can be seen at pore width of 0.2 nm and 1.2 nm respectively while KC5 demonstrated two major peaks at pore width of 0.5 and 1.5 nm. However, these peaks were distributed within the microporous range (pore width < 2 nm). The PSD profiles for KH5 and KC5 has a slight variation in trend as compared to KH2 where several low peaks distributed in the range of 2.5-7.6 nm were observed. All these peaks were

distributed across the wide range mesopores structures (2 nm<pore width<50 nm). This phenomena may probably due to the collapse of pore walls or the aggressive chemical reaction between the activating agent and the adsorbent which results in higher vaporization of organic matter when it was chemically activated at higher chemical concentration thus leading to the widening of the pores [45]. Past researcher had also reported similar results where wider pore structure was obtained when the sample was treated at higher thermal and chemical condition [46, 47].

Table 3 show the detail summary of the textural properties for all four samples. From Table 3, a total surface area of 2, 16, 36 and 189 m^2/g were obtained for KC2, KH5, KH2 and KC5 samples respectively. It was obvious that KC5 sample yield a higher porosity. It is worth to highlight on the results where sample activated at different chemical activating agent and chemical concentration will produce AC with different textural properties. Almost 70-80% of the pores being developed fall in the category of narrow microporosity domain for all four samples. However, the percentage of mesopore obtained in this work can be consider low as compared to the result obtained by past researcher that was also using coffee waste as the precursor for AC production where a mesopore percentage of approximately 53% was reported by Boonamnuayvitaya et al. [48]. The BET surface area as well as the micropore volume obtained in this research work are generally lower as compare to the past research work done by other researchers. Most of the researchers which also used coffee biomass as the precursor for AC production reported a BET surface area within the range of 500–1500 m^2/g [44, 46]. Hence, it is anticipated that there were some limitations during the production of AC as based on the past research done that utilizes coffee biomass, a minimum BET surface area of 500 m^2/g could be achieved.

During the carbonization process in the initial stage of AC production, nitrogen gas was used as an inert gas to eliminate the oxygen content in the horizontal tubular furnace in order to prevent the large ash formation during the heating process. The flow rate used during the carbonization process was 1000 cm^3/min. Studies conducted shows that when gases were flowed at a low flow rate of approximately 50 cm^3/min, the volatile matter being released may not be fully eliminated during the thermal reaction, which results in the re-deposition of volatile matter back to the surface of the sample [49]. Hence, this would lead to the blockage of pore as well as obstructing the development of more pores structure within the sample. Conversely, when the flow rate is too high which is higher than 300 cm^3/min, the surface temperature of the sample would decrease and results to the incomplete removal of volatile matter. Thus, the development of pore structure would be restricted due to the high gas flow rate. This would eventually lead to the low BET surface area of the product formed [49]. Hence, it is suggested to reduce the flow rate to 100 cm^3/min [19].

Table 3. Textural properties for KOH and K_2CO_3 samples.

Carbon Parameters	**KH2**	**KH5**	**KC2**	**KC5**
Total Surface Area, S_{BET} (m^2/g)	36	16	2	189
Total Pore Volume, V_{total} (cm^3/g)	0.0178	0.0100	0.0015	0.0975
Micropores Volume, V_{micro} (cm^3/g)	0.0144	0.0070	0.0011	0.0749
Mesopores Volume, V_{meso} (cm^3/g)	0.0034	0.0030	0.0004	0.0226
Micropores Ratio, V_{micro} (%)	80	70	73	77
Mesopores Ratio, V_{meso} (%)	20	30	27	23

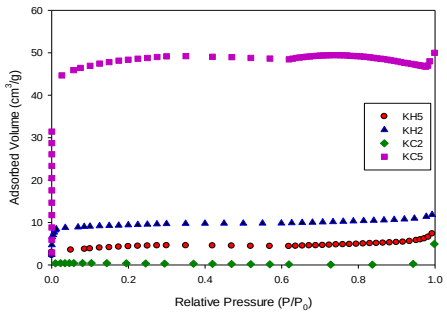

Fig. 4. Adsorption isotherm of N_2 at 77K.

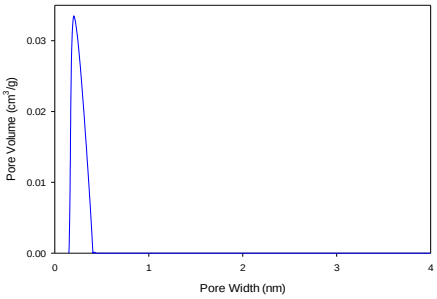

Fig. 5. DFT pore size distribution for KH2.

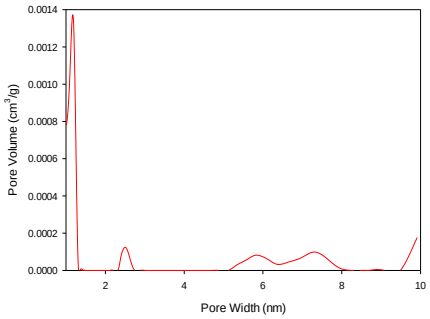

Fig. 6. DFT pore size distribution for KH5.

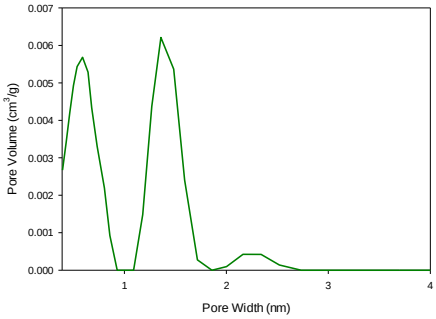

Fig. 7. DFT pore size distribution for KC5.

4. Conclusions

In conclusion, a low cost effective as well as sustainable AC can be developed from raw coffee waste for the application of CCS technology. The study clearly shows the influence of the type of chemical activating agent as well as the chemical concentration used during the activation process on the porosity, surface chemistry and CO_2 adsorption of the resulting AC. From the N_2 isotherm analysis, the results showed that activating agents with different chemical concentration enlarged the surface area and pore structure of the AC in the order of: KC2< KH5< KH2< KC5. Based on the results analysed, it was determined that KC5 sample yielded the highest micropores volume as well as CO_2 adsorption performance with a value of 0.0749 cm^3/g and 2.6 wt. % respectively. This would give a preliminary indication that KC5 would have a better performance for CCS technology. To sum up the whole research, physiochemical activation of the carbon with different chemical agent and concentration gave conclusive results on the formation of microporosity. Based on the results analysed, it was determined that 50 wt. % of K_2CO_3 activation appears to be the most effective route to obtain AC with higher CO_2 adsorption performance. However, in the near future, it is

suggested to reduce the flow rate of gas during the carbonization process to 100 cm^3/min in order to obtained AC with higher BET surface area as well as CO_2 adsorption capacity.

References

1. Zanganeh, K.E.; and Shafeen, A. (2007). A novel process integration, optimization and design approach for large-scale implementation of oxy-fired coal power plants with CO_2 capture. *International Journal of Greenhouse Gas Control*, 1(1), 47-54.
2. Environment Protection Agency (2009). Greenhouse gases threaten public health and the Environment/ Science overwhelmingly shows greenhouse gas concentration at unprecedental levels due to human activity. Retrieved June 7, 2015, from https://www3.epa.gov.
3. Yang, H.; Xu, Z.; Fan, M.; Gupta, R.; Slimane, R.B.; and Bland, A.E. (2008). Progress in carbon dioxide separation and capture: A review. *Journal of Environmental Sciences*, 20, 14-27.
4. Saxena, R.; Singh, V.K.; and Kumar, E.A. (2014). Carbon dioxide capture and sequestration by adsorption on activated carbon. *Energy Procedia*, 54, 320-329.
5. Shibulal, B.; Al-Bahry, S.N.; Al-Wahaibi, Y.M.; Al-Bemani, A.S.; and Joshi, S.J. (2014). Microbial enhanced heavy oil recovery by the aid of inhabitant spore-forming bacteria: An insight review. *The Scientific World Journal*, 2014, 1-12.
6. Feron, P.H.M.; and Hendriks, C.A. (2005). CO_2 capture process principles and costs. *Oil and Gas Science and Technology*, 60, 451-459.
7. Shafeeyan, M.; Ashri, W.; Houshmand, A.; and Shamiru, A. (2010). A review on surface modification of activated carbon for carbon dioxide adsorption. *Journal of Analytical and Applied Pyrolysis*, 89, 143-151.
8. Songolzadeh, M.; Ravanchi, M.; and Soleimani, M. (2012). Carbon dioxide capture and storage: A general review on adsorbents. *World Academy of Science, Engineering and Technology*, 225-232.
9. Khalili, S.; Ghoreyshi, A.A.; and Jahanshahi, M. (2012). Carbon dioxide captured by multiwalled carbon nanotube and activated charcoal: A comparative study. *Chemical Industry & Chemical Engineering Quarterly*, 19(1), 153-164.
10. Din, A.T.M.; Hameed, B.H.; and Ahmad, A.L. (2009). Batch adsorption of phenol onto physiochemical-activated coconut shell. *Journal of Hazardous Materials*, 161, 1522-1529.
11. Hameed, B.H.; Din, A.T.M.; and Ahmad, A.L. (2007). Adsorption of methylene blue onto bamboo-based activated carbon: Kinetics and equilibrium studies. *Journal of Hazardous Materials*, 141, 819-825.
12. Giraldo, L.; and Morena-Pirajan, J.C. (2012). Synthesis of activated carbon mesoporous from coffee waste and its application in adsorption zinc and mercury ions from aqueous solution. *Materials Science*, 9, 938-948.

13. Pradhan, S. (2011). Production and characterization of activated carbon produced from a suitable industrial sludge. Retrieved March 16, 2016, from http://ethesis.nitrkl.ac.in/2630/2/107CH007.pdf.
14. Hamid, S.; Chowdhury, Z.; and Zain, S. (2013). Base catalytic approach: A promising technique for the activation of biochar for equilibrium sorption studies of copper, Cu (II) ions in single solute system. *Materials*, 7(4), 2816-2832.
15. Boonamnuayvitaya, V.; Chaiya, C.; Tanthapanichakoon, W.; and Jarudilokkul, S. (2004). Removal of heavy metals by adsorbent prepared from pyrolyzed coffee residues and clay. *Separation and Purification Technology*, 35, 11-22.
16. Shafeeyan, M.; Daud, W.M.A.W.; Houshmand, A.; and Arami-niya, A. (2012). The application of response surface methodology to optimize the amination of activated carbon for the preparation of carbon dioxide adsorbents. *Fuel*, 94, 465-472.
17. Nabais, J.M.V.; Nunes, P.; Carrott, P.J.M.; Carrott, M.M.L.R.; García, A.M.; and Díaz-Díez, M.A. (2008). Production of activated carbons from coffee endocarp by CO_2 and steam activation. *Fuel Processing Technology*, 89, 262-268.
18. Shafeeyan, M.S.; Daud, W.M.A.W.; Houshmand, A.; and Arami-niya, A. (2011). Ammonia modification of activated carbon to enhance carbon dioxide adsorption: Effect of pre-oxidation. *Applied Surface Science*, 257, 3936-3942.
19. Lee, T.; Zubir, Z.; Jamil, F.; and Matsumoto, A. (2014). Combustion and pyrolysis of activated carbon fibre from oil palm empty fruit bunch fibre assisted through chemical activation with acid treatment. *Journal of Analytical and Applied Pyrolysis*, 110, 408-418.
20. Mohammed, M.; Salmiaton, A.; Azlina, W.W.; and Amran, M.M. (2012). Gasification of oil palm empty fruit bunches: A characterization and kinetic study. *Bioresource Technology*, 110, 628-636.
21. Sharma, R.; Wooten, J.; Baliga, V.; Geoffrey, W.; and Hajaligol, M. (2004). Characterization of chars from pyrolysis of lignin. *Fuel Processing Technology*, 83, 1469-1482.
22. Ballesteros, L.; Cerqueira, M.; Teixeira, J.; and Mussatto, S. (2015). Chracterization of polyssaccharides extracted from spent coffee grounds by alkali pretreatment. *Carbohydrate Polymers*, 127, 347-354.
23. Tsai, W.T.; and Liu, S.C. (2013). Effect of temperature on thermochemical property and true density of torrefied coffee residue. *Journal of Analytical and Applied Pyrolysis*, 102, 47-52.
24. Skreiberg, A.; Skreiberg, O.; Sandquist, J.; and Sorum, L. (2011). TGA and macro-TGA characterization of biomass fuels and fuel mixtures. *Fuel Processing Technology*, 50, 2182-2197.
25. Islam, M.S.; Rouf, M.A.; Fujimoto, S.; and Minowa, T. (2012). Preparation and characterization of activated carbon from bio-diesel by-products (Jatropha seedcake) by steam activation. *Bangladesh Journal of Scientific and Industrial Research*, 47(3), 257-264.

26. Jabit, N. (2007). The production and characterization of activated carbon using local agricultural waste through chemical activation process. Retrieved March 16, 2016, from https://core.ac.uk/download/files/423/11958888.pdf.
27. Raj, B.; and Rao, K.B.S. (2005). Frontiers in materials science. India: Universities Press (India) Private Limited.
28. Rashidi, N.A.; Yusup, S.; and Hameed, B.H. (2013). Kinetic studies on carbon dioxide capture using lignocellulosic based activated carbon. *Energy*, 61, 440-446.
29. Li, W.; Zhang, L.; Peng, J.; Li, N.; Zhang, S.; and Guo, S. (2008). Tobacco stems as a low cost adsorbents for the removal of Pb(II) from wastewater: Equilibrium and kinetic studies. *Industrial Crops and Products*, 28, 294-302.
30. Radosz, M.; Hu, X.; Krutkramelis, K.; and Shen, Y. (2008). Flue-gas carbon capture on carbonaceous sorbents: Toward a low-cost multifunctional carbon filter for "green" energy producers. *Industrial and Engineering Chemistry Research*, 47, 3783-3794.
31. Heidari, A.; Younesi, H.; Rashidi, A.; and Ghoreyshi, A. (2014). Adsorptive removal of CO_2 on highly microporous activated carbons prepared from Eucalyptus camaldulensis wood: Effect of chemical activation. *Journal of the Taiwan Institute of Chemical Engineers*, 45, 579-588.
32. Niya, A.; Daud, W.M.A.W.; and Mjalli, F. (2010). Using granular activated carbon of biomass based activated carbon by phosphoric acid and zinc chloride activation. *Journal of Analytical and Applied Pyrolysis*, 89, 197-203.
33. Ludwinowicz, J.; and Jaroniec, M. (2015). Effect of activating agents on the development of microporosity in polymeric-based carbon for CO_2 adsorption. *Carbon*, 94, 673-679.
34. Namane, A.; Mekarzia, A.; Benrachedi, K.; Belhaneche-Bensemra, N.; and Hellal, A. (2005). Determination of the adsorption capacity of activated carbon made from coffee grounds by chemical activation with $ZnCl_2$ and H_3PO_4. *Journal of Hazardous Materials*, 119, 189-194.
35. Sahira, J.; Mandira, A.; Prasad, P.B.; and Ram, P.R. (2013). Effects of activating agents on the activated carbons prepared from Lapsi seed stone. *Research Journal of Chemical Sciences*, 3, 19-24.
36. Benaddi, H.; Bandos, T.; Jagiello, J.; Schwarz, J.; Rouzaud, J.; and Legras, D. (2000). Surface functionality and porosity of activated carbons obtained from chemical activation of wood. *Carbon*, 38, 669-674.
37. Soleimani, M.; and Kaghazchi, T. (2014). Low-cost adsorbents from agricultural by-products impregnated with phosphoric acid. *Advanced Chemical Engineering Research*, 3, 34-41.
38. Chattopadhyaya, G.; Macdonald, D.; Bakhshi, N.; Mohammadaded, J.; and Dalai, A. (2006). Preparation and characterization of chars and activated carbons from Saskatchewan lignite. *Fuel Processing Technology*, 87, 997-1006.
39. Ahmad, F.; Daud, W.M.A.W.; Ahmad, M.A.; Radzi, R.; and Azmi, A.A. (2013). The effects of CO_2 activation, on porosity and surface functional groups of cocoa (Theobroma cacao) - Shell based activated carbon. *Journal of Environmental Chemical Engineering*, 1, 378-388.
40. Ching, S.L.; Yusoff, M.S.; Aziz, H.A.; and Umar, M. (2011). Influence of impregnation ratio on coffee ground activated carbon as landfill leachate

adsorbent for removal of total iron and orthophosphate. *Desalination*, 279, 225-234.

41. Sevilla, M.; and Fuertes, A. (2011). Sustainable porous carbons with a superior performance for CO_2 capture. *Energy & Environmental Science*, 4, 1765-1771.
42. Hesas, R.; Arami-niya, A.; Mohd, W.; Wan, A.; and Sahu, J. (2013). Preparation and characterization of activated carbon. *Engineering*, 1, 39-50.
43. Sun, N.; Sun, C.; Liu, J.; Liu, H.; Snape, C.E.; Li, K.; Wei, W.; and Sun, Y. (2015). Surface-modified spherical activated carbon materials for pre-combustion carbon dioxide capture. *RSC Advances*, 42, 33681-33690.
44. Reffas, A.; Bernardet, V.; David, B.; Reinert, L.; Lehocine, M.B.; Dubois, M.; Batisse, N.; and Duclaux, L. (2010). Carbons prepared from coffee grounds by H_3PO_4 activation: Characterization and adsorption of methylene blue and Nylosan Red N-2RBL. *Journal of Hazardous Materials*, 175, 779-788.
45. Lee, T.; Ooi, C.H.; Othman, R.; and Yeoh, F.Y. (2014). Activated carbon fibre - The hybrid of carbon fibre and activated carbon. *Review On Advanced Materials Science*, 36, 118-136.
46. Plaza, M.G.; González, A.S.; Pevida, C.; Pis, J.J.; and Rubiera, F. (2012). Valorisation of spent coffee grounds as CO_2 adsorbents for postcombustion capture applications. *Applied Energy*, 99, 272-279.
47. Guo, J.; and Lua, A.C. (2003). Textural and chemical properties of adsorbent prepared from palm shell by phosphoric acid activation. *Materials Chemistry and Physics*, 80, 114-119.
48. Boonamnuayvitaya, V.; Sae-Ung, S.; and Tanthapanichakoon, W. (2005). Preparation of activated carbons from coffee residue for the adsorption of formaldehyde. *Separation and Purification Technology*, 42, 159-168.
49. Lua, A.C.; Lau, F.Y.; and Guo, J. (2001). Preparation and characterization of activated carbon from oil-palm shells. *Sustainable Energy and Environmental Technologies*, 425-429.